A Study on Real-Valued Models for Wideband RF Power Amplifier Modeling

Siqi Wang, Rui Hou, Thomas Eriksson

A Study on Real-Valued Models for Wideband RF Power Amplifier Modeling

Siqi Wang, Rui Hou, *Member, IEEE*, Thomas Eriksson, *Member, IEEE*

***Abstract*—Real-valued Volterra series has been the base of power amplifiers (PA) behavioral modeling. However, most of behavioral models for radio-frequency (RF) PA in the literature are in baseband. In this paper, we make a study on real-valued (RV) models departing from complex-valued memory polynomial (MP) and generalized MP (GMP) for the PA behavioral modeling in RF domain. The proposed RV models are experimentally validated with data measured from a wideband PA.**

***Index Terms*—Behavioral modeling, nonlinearity, RF power amplifiers, real-valued model, Volterra series**

I. Introduction

MULTIPLE signals are required to be simultaneously transmitted in modern wireless communication systems. A wideband power amplifier (PA) which enables the concurrent multi-band transmission can improve both the energy efficiency and the hardware complexity [1]. The behavioral modeling of such a wideband PA needs to describe the nonlinearities and memory effects, which brings non-negligible distortions to the transmitted signals [2].

The Volterra series has been widely used for nonlinear behavioral modeling [3]. In [4], a baseband (BB) equivalent Volterra model is proposed for the PA modeling, which includes the basis functions of memory polynomial (MP) [5], generalized memory polynomial (GMP) [6], dynamic-deviation-reduction (DDR) model [7]. These BB models may be limited in modeling the entire behavior of a wideband PA which in reality receives and transmits signals in radio frequency (RF). In case of a wideband signal transmitted around a carrier frequency in the same order of the band width, as illustrated in Fig. 1, some harmonics and even-order IMDs of some subcarriers fall into the spectrum of the transmitted signal. The classical BB models cannot mimic these behaviors since they only contain odd-order nonlinearities except by adding some specific basis function, which is not a general solution. Therefore, it is important to develop PA behavior models in the RF domain [8].

Siqi Wang was with the Department of Electrical Engineering, Chalmers University of Technology, SE-412 96 Gothenburg, Sweden. He is now with Sorbonne Université, CNRS, Lab. de Génie Electrique et Electronique de Paris, 75252, Paris, France, and Université Paris-Saclay, CentraleSupélec, CNRS, Lab. de Génie Electrique et Electronique de Paris, 91192, Gif-sur-Yvette, France (e-mail of authors: siqi.wang@sorbonne-universite.fr).

Thomas Eriksson is with the Department of Electrical Engineering, Chalmers University of Technology, SE-412 96 Gothenburg, Sweden (e-mail of authors: thomase@chalmers.se).

Rui Hou are with Ericsson AB, Stockholm, Sweden (e-mail of author: rui.hou@ericsson.com).

Color versions of one or more of the figures in this paper are available online at http://ieeexplore.ieee.org.

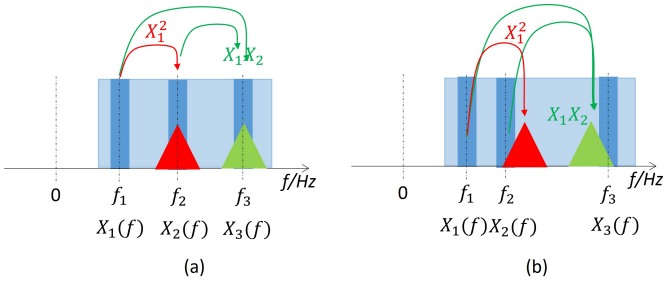

Fig. 1. Even-order IMDs and harmonics due to PA nonlinearity: (a) falling in bands; (b) partially falling in bands.

Both the RF Volterra series and BB complex-valued Volterra model face the challenge of model complexity which increases exponentially when the nonlinearity order or memory depth goes up. In the MP, some "diagonal" terms which contains only a single delay in each basis function are considered the most important and are kept to maintain the modeling accuracy with minimum complexity. In the GMP, some "off-diagonal" terms which allows a second delay in the nonlinearity product in each basis function are added to improve the modeling accuracy. These pruning strategies can also be applied on RF models.

In this paper, we make an analysis on the RF models and develop a real-valued (RV) model for the PA behavioral modeling in the RF domain. We start from an MP model and construct the relation between the RF input and RF output signals. We further expand the analysis from a GMP model and name the obtained equation RF GMP model. Finally, we extract an RV model by simplifying this RF GMP model. The data measured from a real PA are used for experimental validations.

II. Real-valued model of RF signal

A. Conventional PA models

We denote the BB and the digitized RF signals with the same sampling frequency f_s by $x_{\mathrm{BB}}(n)$ and $x_{\mathrm{RF}}(n)$ respectively. The modulation gives $x_{\mathrm{RF}}(n)$ by taking the real part (Re) of $x_{\mathrm{BB}}(n)$ after being upconverted to the carrier frequency f_c:

$$x_{\mathrm{RF}}(n) = \mathrm{Re}\{x_{\mathrm{BB}}(n)e^{j2\pi f_c \frac{n}{f_s}}\}. \tag{1}$$

The demodulation retrieves $x_{\mathrm{BB}}(n)$ by low-pass filtering (LPF) $x_{\mathrm{RF}}(n)$ after being downconverted to DC:

$$\begin{aligned} x_{\mathrm{BB}}(n) &= \mathrm{LPF}\{x_{\mathrm{RF}}(n)e^{-j2\pi f_c \frac{n}{f_s}}\} \\ &= f(n) * \left(x_{\mathrm{RF}}(n)e^{-j2\pi f_c \frac{n}{f_s}}\right), \end{aligned} \tag{2}$$

where $f(n)$ is a low-pass FIR filter of $\mathcal{M}$ taps

$$f(n) = \sum_{m=0}^{\mathcal{M}-1} a_m \delta(n-m). \tag{3}$$

The BB and the digitized RF signals at the PA output are denoted by $y_{\text{BB}}(n)$ and $y_{\text{RF}}(n)$ respectively.

The MP model is a particular case of Volterra series model, which has only the diagonal terms. The commonly used complex-valued MP model can be expressed as following:

$$y_{\text{BBMP}}(n) = \sum_{k=0}^{\mathcal{K}-1} \sum_{l=0}^{\mathcal{L}-1} c_{kl} x_{\text{BB}}(n-l)|x_{\text{BB}}(n-l)|^k \tag{4}$$

where L represents the memory depth and K represents the order of nonlinearity. In [6], the GMP is proposed by incorporating to MP the off-diagonal terms $x_{\text{BB}}(n-l)|x_{\text{BB}}(n-l\pm m)|^k$, where $m > 0$.

B. RF signals in MP

By modulating the output of (4) to RF at f_c, we have

$$\begin{aligned} y_{\text{RFMP}}(n) &= \sum_{k=0}^{\mathcal{K}-1} \sum_{l=0}^{\mathcal{L}-1} \text{Re}\{c_{kl} x_{\text{BB}}(n-l)|x_{\text{BB}}(n-l)|^k e^{j2\pi f_c \frac{n}{f_s}}\} \\ &= \sum_{k=0}^{\mathcal{K}-1} \sum_{l=0}^{\mathcal{L}-1} \text{Re}\{c_{kl} x_{\text{BB}}(n-l) e^{j2\pi f_c \frac{n}{f_s}}\}|x_{\text{BB}}(n-l)|^k \\ &= \sum_{k=0}^{\mathcal{K}-1} \sum_{l=0}^{\mathcal{L}-1} \tilde{c}_{kl} x_{\text{RF}}(n-l)|x_{\text{BB}}(n-l)|^k, \end{aligned} \tag{5}$$

where $\tilde{c}_{kl}$ are real-valued coefficients.

The nonlinearity $|x_{\text{BB}}(n-l)|^k$ can be obtained from $|x_{\text{RF}}(n-l)|^k$ according to (2):

$$\begin{aligned} |x_{\text{BB}}(n-l)|^k &= \left| \sum_{m=0}^{\mathcal{M}-1} a_m \big(x_{\text{RF}}(n) e^{-j2\pi f_c \frac{n-l-m}{f_s}} \big) \right|^k \\ &= \left(\sum_{m=0}^{\mathcal{M}-1} \tilde{a}_m x_{\text{RF}}(n-l-m) \right)^k, \end{aligned} \tag{6}$$

where $\tilde{a}_m = a_m e^{-j2\pi f_c \frac{n}{f_s}}$ are filtering coefficients which keep $\sum_{m=0}^{\mathcal{M}-1} \tilde{a}_m x_{\text{RF}}(n-l-m)$ positive. We can then obtain the expression of the RF MP model from (5):

$$\begin{aligned} y_{\text{RF}}(n) &= \sum_{k=0}^{\mathcal{K}-1} \sum_{l=0}^{\mathcal{L}-1} \tilde{c}_{kl} x_{\text{RF}}(n-l) \left(\sum_{m=0}^{\mathcal{M}-1} \tilde{a}_m x_{\text{RF}}(n-l-m) \right)^k \\ &= \sum_{l=0}^{\mathcal{L}-1} x_{\text{RF}}(n-l) P_{\text{MP}}(n-l), \end{aligned} \tag{7}$$

where

$$\begin{aligned} P_{\text{MP}}(n) = \sum_{k_1=0}^{\mathcal{K}-1} \sum_{k_2=0}^{k_1} \cdots \sum_{k_{\mathcal{M}}=0}^{k_{\mathcal{M}-1}} \bar{c}_{klm} x_{\text{RF}}^{k-k_1}(n) \\ \times x_{\text{RF}}^{k_1-k_2}(n-1) \times \ldots \times x_{\text{RF}}^{k_{\mathcal{M}}}(n-\mathcal{M}+1). \end{aligned} \tag{8}$$

C. RV models

The RF MP model (7) is similar to RF Volterra series in [3] but with less complexity. The kernel $P(n)$ is a k-time inner product of the vector $[x_{\text{RF}}(n), .., x_{\text{RF}}(n-\mathcal{M}+1)]$.

Considering that the complex-valued GMP model in [6] has two off-diagonal branches composed of basis functions as

$$\sum_{k=0}^{\mathcal{K}-1} \sum_{l_1=0}^{\mathcal{L}_1-1} \sum_{l_2=l_1-\mathcal{L}_2}^{l_1+\mathcal{L}_2} c_{kl_1l_2} x_{\text{BB}}(n-l_1)|x_{\text{BB}}(n-l_2)|^k, \tag{9}$$

the corresponding RF GMP model can be extended from (7) as

$$y_{\text{RF}}(n) = \sum_{l_1=0}^{\mathcal{L}_1-1} x_{\text{RF}}(n-l_1) P_{\text{GMP}}(n-l_1), \tag{10}$$

where

$$\begin{aligned} P_{\text{GMP}}(n) = \sum_{l_2=-\mathcal{L}_2}^{\mathcal{L}_2} \sum_{k_1=0}^{\mathcal{K}-1} \sum_{k_2=0}^{k_1} \cdots \sum_{k_{\mathcal{M}}=0}^{k_{\mathcal{M}-1}} \bar{c}_{kl_1l_2m} x_{\text{RF}}^{k-k_1}(n-l_2) \\ \times x_{\text{RF}}^{k_1-k_2}(n-l_2-1) \times \ldots \times x_{\text{RF}}^{k_{\mathcal{M}}}(n-l_2-\mathcal{M}+1). \end{aligned} \tag{11}$$

By omitting off-diagonal terms in $P_{\text{GMP}}(n)$, we can obtain an RV model as:

$$y_{\text{RF}}(n) = \sum_{k=0}^{\mathcal{K}-1} \sum_{l_1=0}^{\mathcal{L}_1-1} \sum_{l_2=\mathcal{L}_0}^{l_1+\mathcal{L}_2} \bar{c}_{kl_1l_2} x_{\text{RF}}(n-l_1) x_{\text{RF}}^k(n-l_2), \tag{12}$$

where $\mathcal{L}_0 = l_1 - \mathcal{L}_2 - \mathcal{M} + 1$.

This RV model can also be expressed in frequency domain to avoid high sampling rate issues:

$$\begin{aligned} Y_{\text{RF}}(\omega) = \sum_{k=0}^{\mathcal{K}-1} \sum_{l_1=0}^{\mathcal{L}_1-1} \sum_{l_2=\mathcal{L}_0}^{l_1+\mathcal{L}_2} \bar{c}_{kl_1l_2} e^{-j2\pi \frac{\omega}{f_s} l_1} X_{\text{RF}}(\omega) \\ * \left(e^{-j2\pi \frac{\omega}{f_s} l_2} X_{\text{RF}}(\omega)^{*k} \right), \end{aligned} \tag{13}$$

where $*$ is the convolution function, and $(\cdot)^{*k}$ represents the convolution power. This frequency domain model can be further extended for digital predistortion (DPD) modeling as in [9]–[11].

III. Experimental results

A. Measurement setup

We use test bench of WebLab [12] for measurements. The BB IQ signal is fed from the PC Workstation to the driver through a Vector Signal Transceiver (PXIe-5646R VST) using a 200 MHz sampling frequency. The VST up-converts the BB signal to the carrier frequency 2.14 GHz. The signal at the output of the PA is then down-converted to baseband by the VST which provides to the PC workstation the BB signal digitized with a sampling frequency of 200 MHz.

A GaN PA CGH40006P transistor mounted in the manufacturer demo-board fabricated by CREE has been used to validate the proposed low rate DPD. Its nominal gain is 13 dB at 2 GHz and the output power at 1dB gain compression is 40.2 dBm.

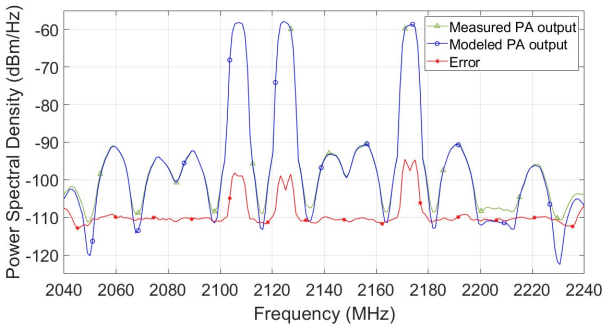

Fig. 2. Output spectra of PA and the proposed real-valued model.

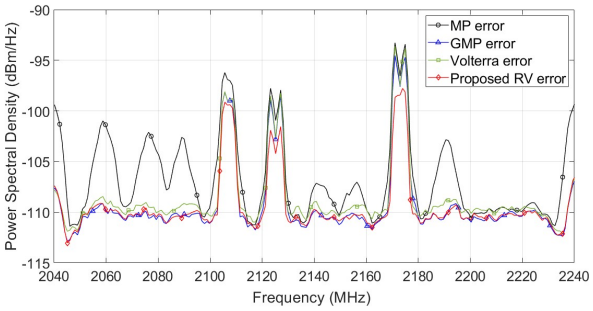

Fig. 3. Spectra of error between modeled and measured PA outputs.

B. Performance of real-valued models

In this section, validation of different complex-valued and real-valued models are given with three different datasets. The parameters of tested real-valued model are: nonlinearity $\mathcal{K} = 7$, main memory depth $\mathcal{L}_1 = 2$, auxiliary memory depth $\mathcal{L}_2 = 4$, filter order $\mathcal{M} = 10$. In Table I, the modeling accuracy as well as the complexity for each model with dual-band, tri-band, and quad-band signals are given. The computational complexity is calculated according to [13] that both a real multiplication and a real addition are counted as 1 flops (floating point operation per sample) while a complex multiplication and addition are counted as 6 and 2 flops. The spectra of measured PA output and GMP model output with tri-band signal as well as their error are given in Fig. 2. The comparison of error spectra between MP, GMP, and Volterra in complex value and in real value is illustrated in Fig.3.

We test the complex-valued MP, GMP and Volterra series to compare with the proposed RV model. The NMSE values in Table I show that the RV model has better accuracy than the MP model, and has much lower complexity than the GMP model and Volterra series.

TABLE I
PERFORMANCE COMPARISON OF DUAL-BAND DPD MODELS

	Baseband modeling			RF modeling
	MP	GMP	Volterra	RV
NMSE of dual-band (dB)	-36.4	-39.0	-38.0	-38.9
NMSE of tri-band (dB)	-36.3	-36.9	-36.9	-37.0
NMSE of quad-band (dB)	-34.7	-37.6	-35.0	-35.1
Number of coefficients	30	270	314	238
Complexity	238	2158	2510	475

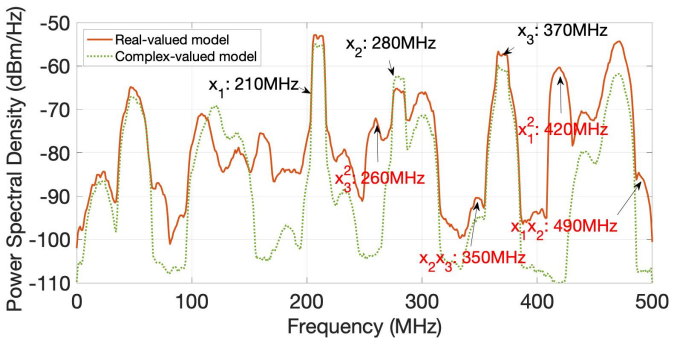

Fig. 4. Simulation of real-valued model with tri-band stimulus.

With the real-valued model (12), we can achieve the same level of NMSE as the complex-valued models. Compared with conventional GMP and Volterra series, the real-valued model (12) has less number of coefficients, which confirms that the most important basis functions are retained in (12).

C. Even-order IMD and harmonics

In Fig.4, we test the real-valued model and the complex-valued model with a tri-band stimulus where the carrier frequencies are 210 MHz, 280 MHz and 370 MHz. We can see that the harmonics and even-order IMDs represented by the real-valued model are absent in the spectrum of complex-valued model output.

The real-valued model is able to mimic all RF behaviors of the PA with any configuration of stimulus, including the harmonics and even-order IMDs. In (7)-(8) and (10)-(11), the carrier frequency information is contained in x_{RF}. The harmonics and even-order IMDs can be generated correctly. From this perspective, the real-valued model is more general than the conventional complex-valued models.

A real-valued DPD can be a future work. Some techniques need to be used to solve the sampling issue. However, the DPD modeling which considers only the used band is much different from the PA modeling which considers the global behavior in the full band. The sampling rate and the computational complexity in a DPD depend much on the total bandwidth of the transmitted signals, as suggested in [14].

IV. Conclusion

In this paper, we present the development of a real-valued model for the PA modeling. Compared with classical complex-valued models, the real-valued model is more accurate for the PA behavioral modeling in wide-band transmission. It has also advantage in complexity since it has only real multiplications and additions. A real-valued DPD can be a future work.

Acknowledgment

This research has been carried out in the LINEAR project, a joint research project financed by Swedish Governmental Agency of Innovation Systems (VINNOVA), Ericsson, and Bluetest.

REFERENCES

[1] E. G. Larsson, O. Edfors, F. Tufvesson, and T. L. Marzetta, "Massive mimo for next generation wireless systems," *IEEE Communications Magazine*, vol. 52, no. 2, pp. 186–195, February 2014.

[2] P. Roblin, C. Quindroit, N. Naraharisetti, S. Gheitanchi, and M. Fitton, "Concurrent linearization: The state of the art for modeling and linearization of multiband power amplifiers," *IEEE Microw. Mag.*, vol. 14, no. 7, pp. 75–91, Nov 2013.

[3] S. Benedetto, E. Biglieri, and R. Daffara, "Modeling and performance evaluation of nonlinear satellite links-a volterra series approach," *IEEE Trans. Aerosp. Electron. Syst*, vol. AES-15, no. 4, pp. 494–507, 1979.

[4] E. G. Lima, T. R. Cunha, H. M. Teixeira, M. Pirola, and J. C. Pedro, "Base-band derived volterra series for power amplifier modeling," in *2009 IEEE MTT-S International Microwave Symposium Digest*, 2009, pp. 1361–1364.

[5] J. Kim and K. Konstantinou, "Digital predistortion of wideband signals based on power amplifier model with memory," *Electronics Letters*, vol. 37, no. 23, pp. 1417–1418, Nov 2001.

[6] D. Morgan, Z. Ma, J. Kim, M. Zierdt, and J. Pastalan, "A generalized memory polynomial model for digital predistortion of RF power amplifiers," *IEEE Trans. Signal Process.*, vol. 54, no. 10, pp. 3852–3860, Oct. 2006.

[7] A. Zhu, J. Pedro, and T. Brazil, "Dynamic deviation reduction-based volterra behavioral modeling of RF power amplifiers," *IEEE Trans. Microw. Theory Techn.*, vol. 54, no. 12, pp. 4323–4332, Dec 2006.

[8] P. L. Gilabert, J.-R. PÃ©rez-Cisneros, Z. Ren, G. Montoro, M. d. L. N. R. LavÃn, and J. A. GarcÃa, "Digital predistortion linearization of a gan hemt push-pull power amplifier for cable applications with high fractional bandwidth," *IEEE Transactions on Broadcasting*, vol. 69, no. 2, pp. 516–527, 2023.

[9] A. Brihuega, L. Anttila, and M. Valkama, "Frequency-domain digital predistortion for ofdm," *IEEE Microw. Wireless Compon. Lett.*, vol. 31, no. 6, pp. 816–818, 2021.

[10] S. Wang, P. Maris Ferreira, and A. Benlarbi-Delai, "Physics informed spiking neural networks: Application to digital predistortion for power amplifier linearization," *IEEE Access*, vol. 11, pp. 48 441–48 453, 2023.

[11] A. Brihuega, L. Anttila, and M. Valkama, "Beam-level frequency-domain digital predistortion for ofdm massive mimo transmitters," *IEEE Transactions on Microwave Theory and Techniques*, vol. 71, no. 4, pp. 1412–1427, 2023.

[12] P. N. Landin, S. Gustafsson, C. Fager, and T. Eriksson, "Weblab: A web-based setup for PA digital predistortion and characterization [application notes]," *IEEE Microw. Mag.*, vol. 16, no. 1, pp. 138–140, Feb 2015.

[13] A. S. Tehrani, H. Cao, S. Afsardoost, T. Eriksson, M. Isaksson, and C. Fager, "A comparative analysis of the complexity/accuracy tradeoff in power amplifier behavioral models," *IEEE Trans. Microw. Theory Techn.*, vol. 58, no. 6, pp. 1510–1520, June 2010.

[14] S. Wang, W. Cao, R. Hou, and T. Eriksson, "A digital predistortion for concurrent dual-band power amplifier linearization based on periodically nonuniform sampling theory," *IEEE Trans. Microw. Theory Tech.*, vol. 70, no. 1, pp. 466–475, 2022.